F. Ferrari, M. Lavagna
Suitable Configurations for Triangular Formation Flying About Collinear Libration Points Under the Circular and Elliptic Restricted Three-Body Problems
Acta Astronautica, Vol. 147, 2018, p. 374-382
doi:10.1016/j.actaastro.2016.08.011

Suitable Configurations for Triangular Formation Flying about Collinear Libration Points under the Circular and Elliptic Restricted Three-Body Problems

Fabio Ferrari*, Michèle Lavagna

Department of Aerospace Science and Technology, Politecnico di Milano, Via La Masa 34, Milan, 20156, Italy.

Abstract

The design of formations of spacecraft in a three-body environment represents one of the most promising challenges for future space missions. Two or more cooperating spacecraft can greatly answer some very complex mission goals, not achievable by a single spacecraft. The dynamical properties of a low acceleration environment such as the vicinity of libration points associated to a three-body system, can be effectively exploited to design spacecraft configurations able of satisfying tight relative position and velocity requirements. This work studies the evolution of an uncontrolled formation orbiting in the proximity of periodic orbits about collinear libration points under the Circular and Elliptic Restricted Three-Body Problems. A three spacecraft triangularly-shaped formation is assumed as a representative geometry to be investigated. The study identifies initial configurations that provide good performance in terms of formation keeping, and investigates key parameters that control the relative dynamics between the spacecraft within the three-body system. Formation keeping performance is quantified by monitoring shape and size changes of the triangular formation. The analysis has been performed under five degrees of freedom to define the geometry, the orientation and the location of the triangle in the synodic rotating frame.

Keywords: CR3BP, ER3BP, Relative Dynamics, Formation Flying, Triangular Formation, Multi-Body Dynamics

*Corresponding author. Tel.: +39 02 23998428

Email addresses: fabio1.ferrari@polimi.it (Fabio Ferrari), michelle.lavagna@polimi.it (Michèle Lavagna)

1. Introduction

The dynamics of spacecraft flying in formation in the proximity of libration points associated to a three-body system represents one of the most promising research field for future space mission design. The convenient properties of three-body dynamics combine to the design flexibility of having more than one spacecraft. Many scientific fields find possible applications and benefit from this peculiar coupling: observation and basic science, from telecommunications to space exploration. When designing classical formations of spacecraft, the cost to be paid is the resolution of a highly challenging trajectory and station keeping problem solving, to satisfy tight requirements on relative dynamics between each member of the formation. The exploitation of low acceleration regions such as the proximity of equilibrium points associated to a three-body system opens to a wide range of design opportunities, and three-body dynamics can be conveniently used to reduce such trajectory and station keeping needs.

The problem of formation flying has been extensively studied in the past decades and many missions employing such architecture have been designed. However, not many concepts of formations of spacecraft have been designed to exploit three-body dynamics. Several studies aimed to the design of control strategies for formations of spacecraft under a three-body dynamics exist, but very few of them studies the free relative motion between the spacecraft as they are subjected to this highly unstable and non-linear environment. Among them, Barden and Howell[1] exploited the natural motion on the center manifold near periodic orbits to reproduce tori of quasi-periodic trajectories that can be useful for the design of naturally bounded formations of spacecraft. Few years later, Gómez, Marcote, Masdemont and Mondelo[2] derived regions around periodic orbits with zero relative velocity and radial acceleration, which ideally keep unchanged the relative distances between the spacecraft in the formation. Finally, Héritier and Howell[3] extended the analysis done by Gómez et al. and derived low drift regions (low relative velocity and acceleration) around periodic orbits, as quadric surfaces. Ferrari and Lavagna[4] generalized the work by Héritier and Howell to the whole three-body domain, identifying regions of zero relative acceleration and velocity (ZRAV loci) for large formations of spacecraft. Also, the relative dynamics of a three-spacecraft triangular formation have been investigated and suitable

initial conditions have been found in the Earth-Moon system.[4] Controlled formations have been studied under the Elliptic Restricted Three-Body Problem (ER3BP) formulation[5] but still there is very little known about the free relative dynamics within this particular dynamical environment.

A three spacecraft triangularly-shaped formation is assumed as a representative geometry to be studied. One example of such a formation arrangement is the LISA mission,[6] which consists of three identical spacecraft, placed around a reference point that orbits the Sun, following a circular path. Other examples of similar configurations are given by Cluster II[7] and Magnetospheric Multiscale Mission (MMS):[8] both of them employ a tetrahedral (triangular pyramid) formation to study Earth's magnetosphere.

Configurations providing good performance in terms of formation keeping, have been investigated and key parameters, which mainly control the formation dynamics within the three-body system, have been identified. Formation keeping performance is quantified by defining performance indexes to monitor shape and size changes of the triangular formation and to compare them against the desired dynamical behavior of the formation. Some constraints are imposed to the relative dynamics within the formation and the best solution, in terms of free and uncontrolled dynamics is identified within a specific set of initial conditions. The analysis has been performed under several degrees of freedom to define the geometry, the orientation and the location of the triangle in the synodic rotating frame: one parameter defines the size of the triangle and five parameters describe unequivocally its location and orientation in the rotating frame. The solution is provided in terms of initial configuration of the formation which fits at best the constraint imposed on the formation dynamics. The best initial configurations, which maximize performance indexes, are found after Monte Carlo simulations.

2. Dynamics

The dynamics of the spacecraft are described by using three-body models. The Circular and Elliptic Restricted Three-Body Problem formulations (respectively CR3BP and ER3BP) are used. The equations of motion and peculiar periodic solutions associated to these dynamical models, in use in this work, are briefly recalled here.

2.1. The Circular Restricted Three-Body Problem

The CR3BP is used to describe the motion of a third body, which moves under the gravitational attraction of two main massive bodies, called primaries (M_1, M_2). The motion of the third body is influenced by the attraction of the primaries but it does not influence their motion. The primaries follow a two-body solution about their common center of mass. In the CR3BP the primaries are constrained to move on circular orbits. It is useful to express the equations of motion of the third body in a reference frame $(x, y, z)_{\text{rot}}$ which is centered in the center of mass of the two primaries and rotates together with them with angular velocity ω (Figure 1).

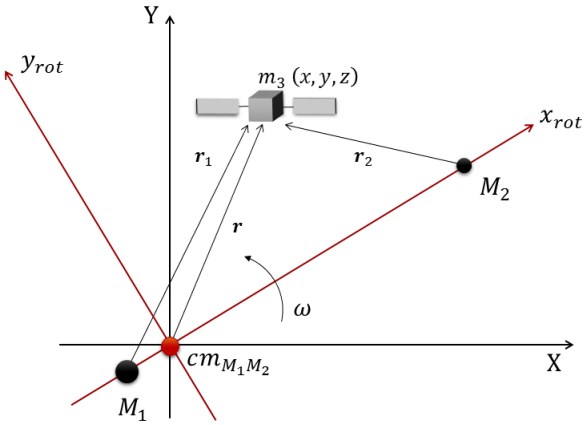

Figure 1: Three-body synodic frame

The equations of motion can be conveniently written in a nondimensional form, using the potential function associated to the problem

$$U = \frac{1}{2}(x^2 + y^2) + \frac{1-\mu}{r_1} + \frac{\mu}{r_2} \tag{1}$$

with

$$r_1 = \sqrt{(x+\mu)^2 + y^2 + z^2} \tag{2a}$$

$$r_2 = \sqrt{(x-(1-\mu))^2 + y^2 + z^2} \tag{2b}$$

The parameter μ is called mass ratio and it is defined as follows

$$\mu = \frac{M_2}{M_1 + M_2} \tag{3}$$

The equations of motion read as

$$\begin{cases} \ddot{x} - 2\dot{y} = U_x \\ \ddot{y} + 2\dot{x} = U_y \\ \ddot{z} = U_z \end{cases} \tag{4}$$

where the notation $U_{(\cdot)}$ means partial derivative of the potential with respect to the variable $(\cdot)$.

2.1.1. Lyapunov families in the CR3BP.

Infinite possibilities, in terms of periodic solutions, are known to exist when considering the Circular Restricted Three-Body Problem. The present work studies the free dynamics of formation of satellites about collinear libration points when the barycenter of the formation is initially placed on a periodic orbit, named *reference orbit*. Among the many possibilities, reference orbits in the CR3BP have been chosen among Lyapunov families about the Earth-Moon L1, L2 and L3 points. Figure 2 shows families of Lyapunov orbits about the collinear libration points. Note that these orbits represent planar solutions since they belong to the (x, y) plane.

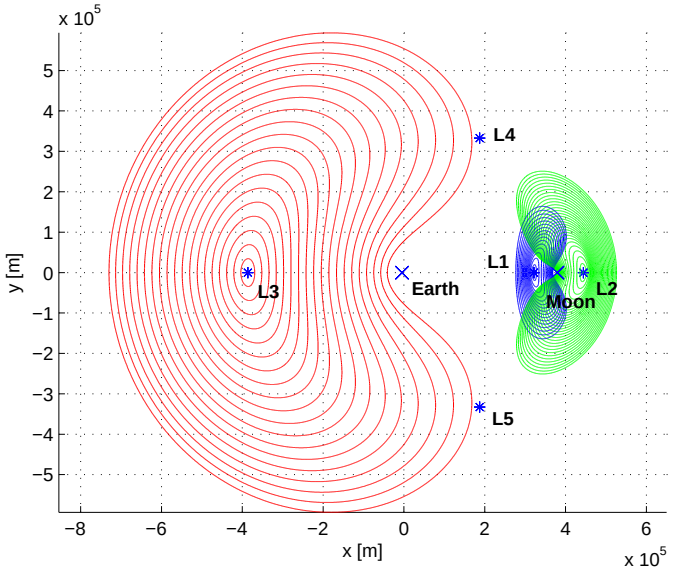

Figure 2: Lyapunov families about collinear libration points in the Earth-Moon system

2.2. The Elliptic Restricted Three-Body Problem

The assumption of primaries following circular paths about the center of mass of the system fits well if the eccentricity of their two-body solution is zero or very small. In general, this assumption represents a simplification and in some cases (when eccentricity is high) it leads to large errors affecting the motion of the third body. The ER3BP avoids the simplification of the circular case, since the primaries follows elliptical paths about their common center of mass.

Unlike the CR3BP, the position of the primaries is not fixed in the rotating frame. Since they move along elliptical orbits, their relative distance ρ is not constant in time and depends on the instantaneous position of the primaries, through the true anomaly f

$$\rho = \frac{p}{1 + e\cos f} \tag{5}$$

where p is the semi-latus rectum and e is the eccentricity of the primaries orbit. As result, when seen from the rotating frame, the position of the primaries pulsates along the x axis. The equations of motion are then written in a rotating-pulsating reference frame.

In analogy to the CR3BP, the equations of motion are usually written in a nondimensional form,[9] using the pseudo-potential function associated to the problem[10]

$$U = \frac{1}{1 + e\cos f}\left[\frac{1}{2}(x^2 + y^2 - z^2 e\cos f) + \frac{1-\mu}{r_1} + \frac{\mu}{r_2}\right] \tag{6}$$

where r_1 and r_2 represent the distance of the particle from the primaries, while μ is the mass ratio of the planetary system.

The equations of motion are written as

$$\begin{cases} x'' - 2y' = U_x \\ y'' + 2x' = U_y \\ z'' = U_z \end{cases} \tag{7}$$

Unlike in (4), the equations of motion do not express time derivatives, but $(\cdot)'$ and $(\cdot)''$ indicate first and second derivative with respect to the true anomaly, while the notation $U_{(\cdot)}$ indicates the partial derivative of the pseudo-potential with respect to the variable $(\cdot)$. An important consequence when introducing a nonzero eccentricity of the primaries is that the system (7) is non-autonomous, since the right-hand terms explicitly depend on time: the motion of the third body depends on the position of the primaries.

2.2.1. Periodic orbits in the ER3BP.

The CR3BP is known to have infinite periodic solutions which can be collected into families of orbits with continuously varying period. When the problem is generalized to the elliptic one, this is not valid anymore: the ER3BP admits only isolated periodic orbits, with well-determined periods. This is due to the fact that the motion of the particle depends explicitly on time, i.e. on the location of the primaries. Since the time-dependent terms in (7) are periodic with period 2π (one revolution of the primaries between their common center of mass), then periodic solutions of the ER3BP must be periodic of period $T = 2\pi N$, with $N = 1, 2, \ldots$. Periodic orbits in the ER3BP, in use in this work, have been generated starting from nearly resonant orbits in the CR3BP, through eccentricity continuation techniques. Examples of how periodic orbits can be computed can be found in[11] and.[12]

3. Statement of the problem

This section presents the problem addressed, showing how numerical simulations have been set within the domain of validity of the study. As mentioned, the study focuses on the free dynamics of a formation of satellites, with the goal to find suitable initial configurations leading to good performance in terms of formation keeping. In the present section, the reader will find explanation to what is referenced with the term *initial configuration* and to what is meant by formation keeping performance. In addition, criteria driving the selection of suitable initial configurations will be defined and motivated.

3.1. Initial condition set

Three identical spacecraft are located at the vertexes of an equilateral triangle. The initial configuration of the formation is specified by a set of parameters representing the initial size and orientation of the triangle.

Figure 3 shows a possible initial configuration of the formation with respect to the local frame, which is centered in the barycenter of the formation and defined such that x, y and z are directed as the axes of the three-body synodic frame. The initial size of the triangle is identified by the parameter d, which represents the distance between each spacecraft and the barycenter of the equilateral triangle. The initial orientation of the formation is found using the vector normal to the triangle plane $\boldsymbol{n}$ and the angle γ which

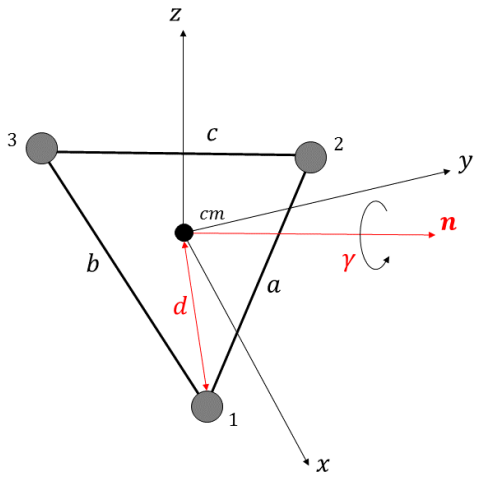

Figure 3: Triangular formation in the local frame

represent positive rotation about $\boldsymbol{n}$ axis as shown in Figure 3. Five parameters are used to unequivocally define the geometry and the orientation of the formation in the rotating frame. Finally, the reference orbit has to be chosen. Summarizing, to define the initial configuration of the formation the following parameters shall be fixed:

- d: distance between each spacecraft and the center of mass of the formation
- $\boldsymbol{n}$: normal to the triangle plane (three-component unity vector)
- γ: rotation about $\boldsymbol{n}$ axis
- X_{ref}: reference orbit (initial conditions)

Once the initial configuration has been selected, that is the selection of initial state of the three spacecraft, the equations of motion are integrated forward in time for each spacecraft as they evolve near the reference trajectory. The evolution of the formation is monitored. The aim of the study is to investigate the effect that different initial configurations have on the relative dynamics between the three spacecraft and to identify the best cases.

3.2. Performance factors

The ideal formation keeping condition can be synthesized with no change in shape and size of the initial triangular configuration as the spacecraft fly near the reference orbit. The ideal condition is, of course, impossible to obtain if the formation is free and uncontrolled, in the extremely chaotic and non-linear three-body environment. Nonetheless, it is possible to seek preferred initial configurations which lead to small changes in shape and size of the formation, that is cheaper formation keeping needs. In order to evaluate how the formation is maintained, it is important to study how the shape and the size of the triangular formation change during the evolution of the three spacecraft along the orbit. It is useful to define a way to measure formation keeping performance, trying to quantify both shape and size changes. This way, it would be possible to identify initial conditions sets leading to good formation keeping maintenance. To this purpose, two performance factors are used: the *Shape Factor* (SF), taking into account for the change in the shape of the triangle, and the *Size* or *Dimension Factor* (DF), taking into account for the change in size of the triangular formation. These performance indexes have been introduced by the authors in a previous work,[4] where the interested reader can find more details about their mathematical definitions. The following paragraphs recall the analytical expressions of the two indexes.

3.2.1. Shape Factor.

The Shape Factor (SF) is defined as

$$SF = e^{-\sqrt{(\ln \varepsilon_1)^2 + (\ln \varepsilon_2)^2}} \tag{8}$$

with

$$\varepsilon_1 = \frac{a}{b} \qquad \varepsilon_2 = \frac{a}{c} \tag{9}$$

where a, b and c represent the current length of the sides of the triangle at a generic time t, with reference to Figure 3. Note that the SF is a nondimensional variable that ranges from 0 to 1. It can be easily verified that the shape is unchanged if and only if

$$\varepsilon_1 = \varepsilon_2 = 1 \tag{10}$$

and then the ideal condition of unchanged shape is

$$SF = f(\varepsilon_1, \varepsilon_2) = f(1, 1) = 1 \tag{11}$$

Figure 4 shows the 3D graphics of Equation (8), which represents the Shape Factor function.

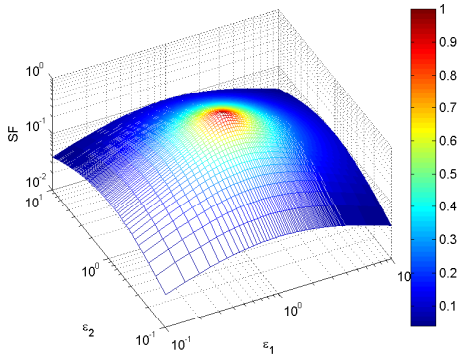

Figure 4: Shape Factor (logarithmic scale)

3.2.2. Dimension Factor.

The Size or Dimension Factor (DF) monitors the size of the triangle during the evolution of the formation and it is defined as

$$DF = \frac{\eta_1 + \eta_2 + \eta_3}{3} \tag{12}$$

with, referring to Figure 3

$$\eta_1 = \frac{a}{a_0} \qquad \eta_2 = \frac{b}{b_0} \qquad \eta_3 = \frac{c}{c_0} \tag{13}$$

Note that this index is also nondimensional but here the ratios are computed for each side, with respect to its initial length, denoted by subscript $_0$. The DF equals one only at the initial time and when the average size of the formation is maintained. Differently from the SF, it needs information on the initial state of the formation and provides a measure of the size of the triangle at a certain time after initial time. Roughly speaking, DF=3 at $t = t_1$ (with $t_1 > t_0$) means that the triangle is, on average, three times bigger than its initial size at $t = t_0$.

3.3. Simulated scenarios

To find good initial configurations, a simulation campaign has been set up and several initial configurations have been explored. The initial orientation of the triangle, the initial size of the formation (d) and the reference orbit are the free parameters investigated. The study is split into two parts. The

first part investigates the most general behavior, considering many different initial conditions sets in the CR3BP and it is referred as *general analysis*. The second part considers only the subset of initial conditions sets domain corresponding to the best solutions found as output to the general analysis and studies them in deep using the more accurate ER3BP.

The order of magnitude of the size of the formation d has been chosen by analogy with existing missions employing similar formation configurations: for example, the size of Cluster II[7] and MMS[8] formations varies from few kilometers up to few thousands of kilometers. For the general analysis, the simulation campaign has been set up by considering the $d = 1, 10, 100$ km. For what concerns the orbital path of the spacecraft, the study has been performed by considering only planar reference orbits. In particular, the following Lyapunov orbits about L1, L2 and L3 of Earth-Moon system have been used:

L1	$Ay =$ 8246,	44582,	88339	km
L2	$Ay =$ 7334,	75019,	145740	km
L3	$Ay =$ 6874,	100719,	338888	km

where Ay represents the maximum semi-amplitude of the orbit in the y direction. In the followings, the orbits will be referenced as L1(1), L1(2), L1(3), L2(1), L2(2),... where the numbers in the brackets indicates which orbit, from the smallest (1) to the largest (3), is being referenced. For example, L3(2) refers to the intermediate orbit about L3 with $Ay = 100719$ km. Figure 5 shows a plot of the orbits used as reference, in the Earth-Moon rotating frame.

The barycenter of the formation is placed on the reference orbit, the state of the three spacecraft is integrated forward and the time evolution of the triangle is monitored during one period of the reference orbit. Overall, three sizes d of the formation, nine reference orbits and many initial orientations of the formation with respect ot the rotating frame have been considered.

To find suitable initial conditions in terms of formation keeping, the behavior of the previously defined performance factors is studied to find the closest conditions to the ideal situation (no change in shape and size of the formation), which is given by

$$SF = 1 \qquad DF = 1 \tag{14}$$

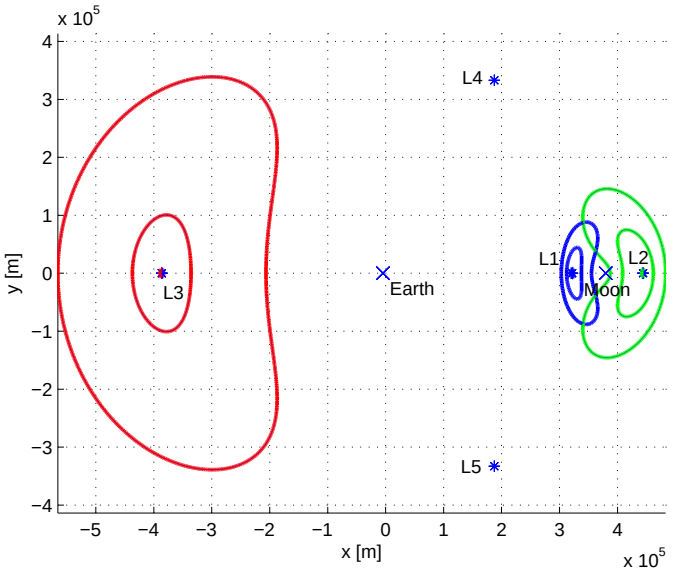

Figure 5: Reference Lyapunov orbits in the Earth-Moon system (general analysis)

4. Results

The best initial configurations, limited to the domain of parameters defined in the previous section, have been found.

Figures 6(a) and 6(b) show examples of how performance factors behave in time during the evolution of the formation on the reference orbit: figures refers to a formation flying about the reference orbit L3(3), with $d = 10$ km. Performance factors have been evaluated for different orientations. In this case, with reference to Figure 3, angles refer to simple rotations about the x axis, that is $\boldsymbol{n}$ directed towards the positive x axis, and with γ representing a rotation about it. Rotations are here computed starting from $\gamma = 0$, found when one spacecraft is along the positive z axis and the remaining two are below the (x, y) plane. Nondimensional time is shown on the abscissa, referring to the percentage of orbital period of the reference orbit (the time span goes from 0 to one period T_{orb}).

To compare different initial conditions sets, the value of the performance factors is evaluated after one period of the reference orbit. The functions in Figures 6(a) and 6(b) have been evaluated at $t = T_{orb}$ for any different initial orientation and size d of the formation and for any of the selected reference orbits.

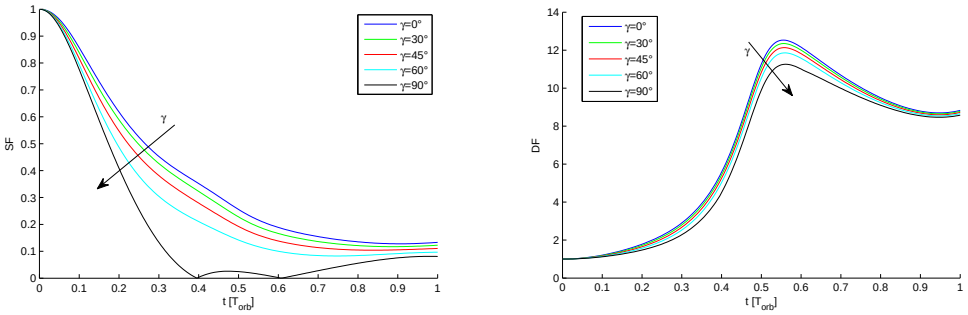

(a) (b)

Figure 6: Time evolution of (a) Shape Factor and (b) Dimension Factor for different initial orientations (L3(3) reference orbit, $d = 10$ km, rotation angle about the x axis)

4.1. General analysis in the CR3BP

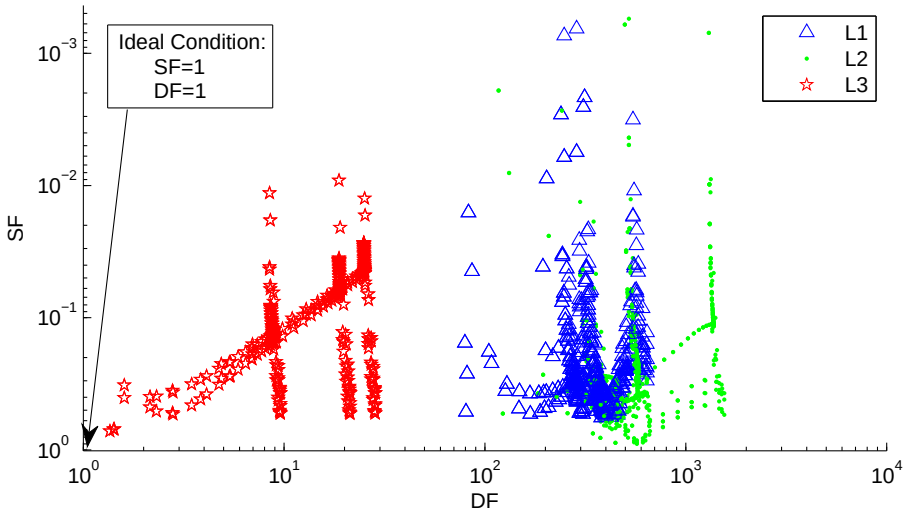

Figure 7: Totality of solutions (limited to the case of study)

Interesting results can be obtained by comparing all simulated scenarios. Figure 7 shows the outcome of the simulation campaign. The value of performance factors after one period has been computed for any possible case: each set of parameters is represented by a point in the SF-DF plane. Note that DF increases on the abscissa, while SF decreases on the ordinate: the

ideal formation keeping condition is then located at the left-bottom corner of the graph, where both performance factors equal one. The best conditions must be sought then in the left/lower region of the plot.

Blue triangles represent solutions associated to formations orbiting L1, green dots are associated to formations orbiting L2 and red stars to formations orbiting L3. The first thing to be noticed is that there are big differences in terms of final size of the formation (DF) depending on the libration point the reference orbit is about. L3 orbits represent by far the best place to host a formation of satellites: all solutions related to L3 orbits exhibit a lower DF then any other solution about L1 or L2. Looking at numbers, the final value of DF is always lower than 25 if L3 orbits are considered, while it is always greater than 80 for L1 orbits and it is always greater than 120 for L2 orbits. For what concern formation keeping, the orbits considered here about L1 and L2 are not then good candidates to host a triangular formation of satellites, since after one orbital period the size of the triangle increases dramatically and the spacecraft lose their initial relative configuration.

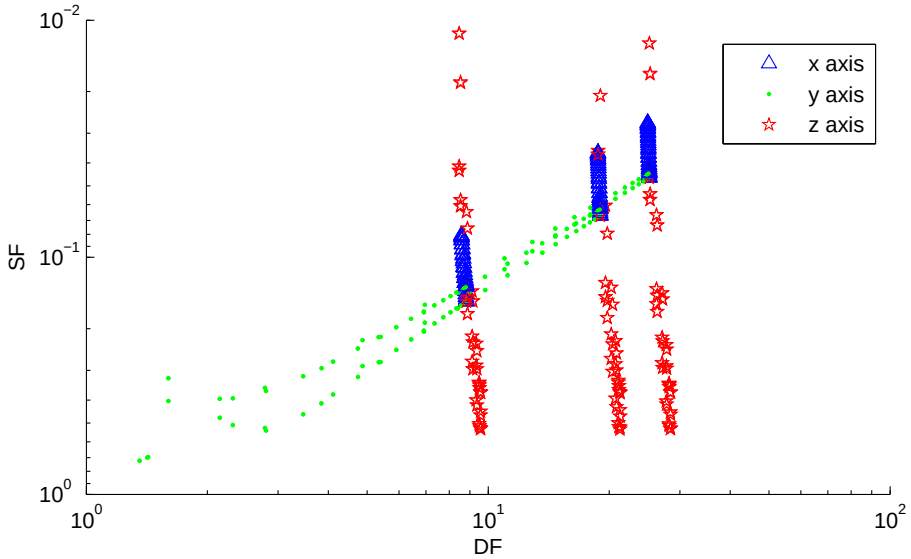

Figure 8: Solutions associated to L3 orbits (formation plane normal to x, y, z axes)

Discarding all solutions related to L1 and L2 orbits, the analysis can be focused on L3 orbits. Figure 8 show an enlargement of Figure 7, considering only solutions associated to L3 orbits. Here some interesting patterns can

be identified, when looking at simple rotations, i.e. when the normal to the formation plane is directed towards x, y or z axes. Blue triangles represent cases with normal directed as the x axis, green dots are associated to formation plane normal to the y axis and red stars to cases with normal towards the z axis. Each different point is associated to a different value of rotation angle γ (from 0 to 2π), initial size of the formation d and initial orbit about L3. The figure shows that the best performance is achieved when considering the plane of the formation normal to the y axis, that is when $\boldsymbol{n}$ is directed towards y axis.

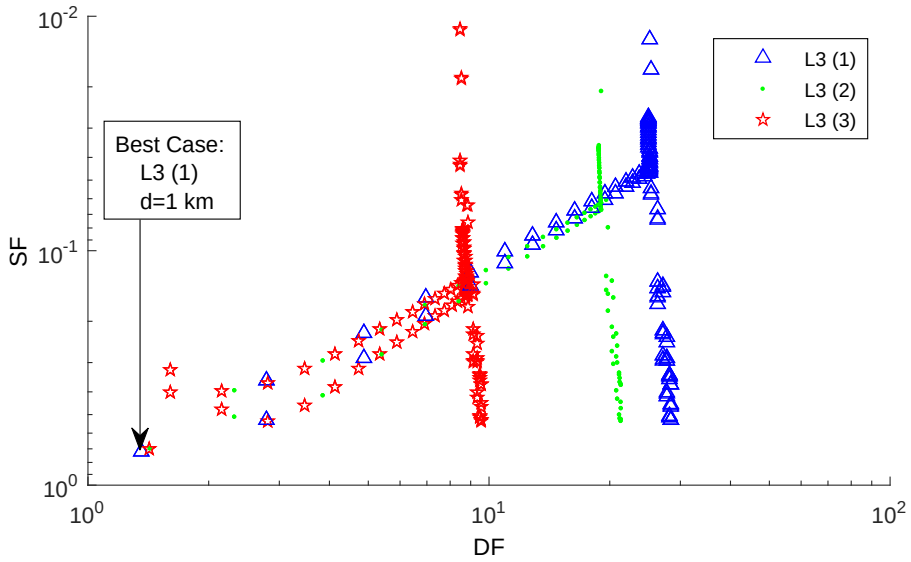

Figure 9: Solutions associated to L3 orbits (according to the reference orbit)

Figure 9 shows the same solutions (considering only L3 orbits) but highlighting the effect of the different reference orbit (small to large orbits about L3). The selection of the orbit produces different results in terms of DF values: the bigger the orbit, the smaller the maximum DF experienced by the formation. However, while being true for the maxima, this is not true for the DF minima since the overall best case is found for a formation flying about the smallest orbit about L3.

For what concern the initial size of the formation, no relevant effects have been observed for the different d values investigated.

4.2. Simulation campaign about L3 in the ER3BP

The important result coming out from general analysis is that best formation keeping performance is achieved for formations in L3. This section wants to study in deep the dynamical behavior in this region. A Monte Carlo simulation campaign has been set up and several initial configurations of formations in L3 have been explored. In particular, different initial orientations of the triangle $(\boldsymbol{n}, \gamma)$ and different initial sizes of the formation (d) have been considered. In this second study, the simulation campaign has been set up by considering the following values to initialize the size of the formation:

$$d = 10^N \text{ m} \quad \text{with} \quad N = 0, 1, 2, \ldots, 8$$

meaning that the size of the triangle varies from a minimum of 1 m up to a maximum of 10^5 km.

The orientation of the formation has been generated randomly, with a uniform spherical distribution. Figure 10 shows the distribution associated to the orientation of the triangle. Each point in Figure 10 represents a different orientation of the formation: the normal to the triangle $\boldsymbol{n}$ corresponds to the vector joining the origin of the reference frame to the point on the sphere, which is also centered in the origin. In this work 10^4 points have been used to generate initial conditions for vector $\boldsymbol{n}$.

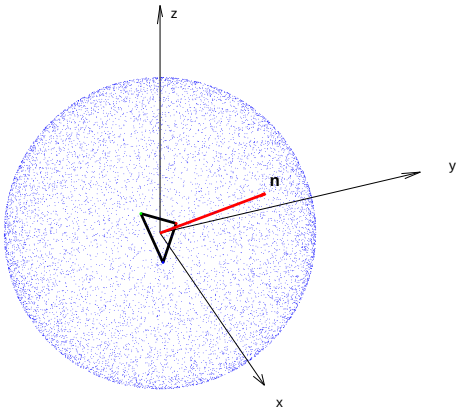

Figure 10: Orientation of the formation, uniform spherical distribution to set up Monte Carlo simulation (10^4 points)

For each $\boldsymbol{n}$ case, different values of angle γ have been considered, ranging between 0 and 360°, with an incremental value of 5°. This leads to 72 different values of γ for each normal vector to the triangle plane.

Summarizing, the simulation scenario includes 9 different initial sizes of the formation, 10^4 different normal vectors to the triangle plane and 72 different rotation angles γ, for a total amount of 9 x 10^4 x 72 = 6.48 millions of different cases simulated.

4.2.1. Reference orbit.

The analysis has been performed by considering the reference orbit in Figure 11. It represents a resonant periodic orbit with one-year period about L3 in the Sun-Earth system. From the numerical point of view, the orbit has been found starting from a resonant 1:1 orbit in the CR3BP about L3, through eccentricity continuation. The maximum amplitude of the orbit in the y and z directions are

$$\Delta y = 3.88 \cdot 10^8 \quad \text{km}$$
$$\Delta z = 3.39 \cdot 10^4 \quad \text{km}$$

Note that the out-of-plane amplitude (z) is significantly lower than amplitude in x and y directions: for this reason the orbit is here classified as a quasi-planar Halo orbit.

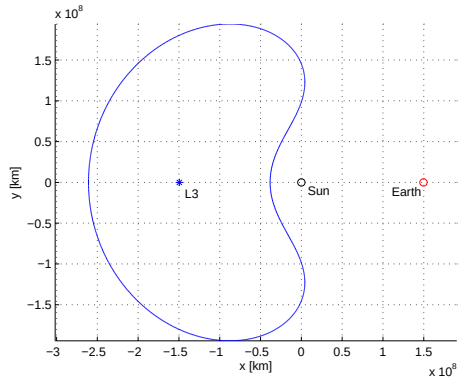

Figure 11: Reference orbit

4.3. Results of simulations about L3

After collecting SF and DF performance for each different set of parameters, it is possible to look at aggregated results, to identify the best initial configurations.

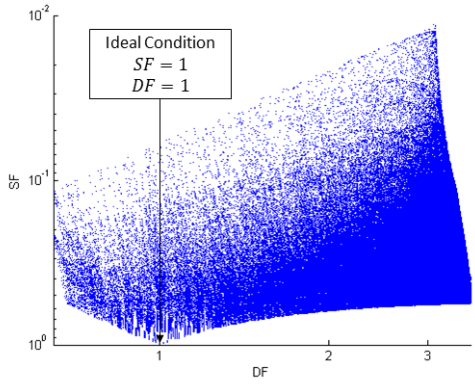

Figure 12: Solutions for $d = 1$ km (72 x 10^4 points)

Figure 12 shows the results for $d = 1$ km. Each set of initial conditions (72 x 10^4 different sets in this case) is represented by a point in the SF-DF plane. The coordinates of each point represent the value of SF and DF after integrating the equations of motion starting from that particular set of initial conditions, for one period of the reference orbit. Note that DF increases on the abscissa, while SF decreases on the ordinate: the ideal formation keeping condition is pointed by the arrow in figure, where both performance factors equal one. Suitable configurations must be sought in the proximity of that point.

For what concern the initial size of the formation, no relevant effects have been observed for the different d values explored. Aggregated results associated to different d values looks very similar between them and when compared to Figure 12. The identification of the best case between different sets of results shows also very little dependence on the parameter d. It can be then concluded that, under the domain investigated in this work, the initial size of the formation has no relevant effect on the relative dynamics between spacecraft in the proximity of the chosen reference trajectory. This result agrees with the results of the general analysis performed under the CR3BP formulation.

4.4. Best case

Since no relevant effect are observed with respect to the size of the triangle, formation keeping performance depends mainly on the initial orientation

of the triangle plane $(\boldsymbol{n}, \gamma)$. The first step is to identify convenient solutions in terms of $\boldsymbol{n}$, that is the normal unity vector to the triangle surface.

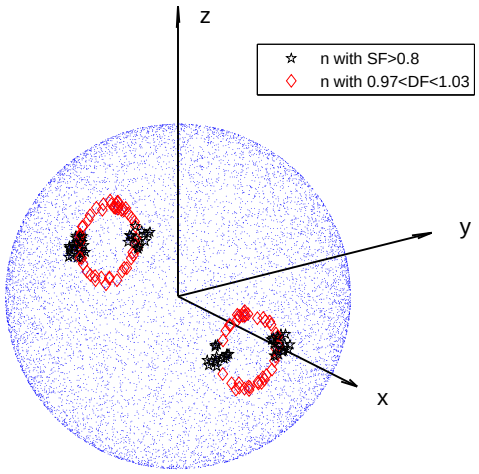

Figure 13: $\boldsymbol{n}$ ensuring highest performance

Figure 13 shows regions on the overall distribution sphere where $\boldsymbol{n}$ (vector joining the origin with point on the sphere) leads to $SF < 0.8$ (black stars) or to a DF between 0.97 and 1.03 (red diamonds). The intersections between these regions correspond to the points in the neighborhood of the ideal point in Figure 12. Note that as far as the cases highlighted by Figure 13 are concerned, the triangle lies on the y, z plane or slightly inclined with respect to it. This is in agreement with the results of the analysis carried in the circular problem.[4]

Figure 14 shows the overall best case, achieved when the $\boldsymbol{n}$ unity vector is directed towards the x axis, that is when the triangular formation lies initially on the y, z plane. For what concern the last parameter (γ), a brief analysis showed that the best performance is always achieved when one of the spacecraft lies on the (positive or negative) y axis of the rotating frame.

This initial configuration leads to values of SF and DF after one period of

$$SF = 0.98$$
$$DF = 1.02$$

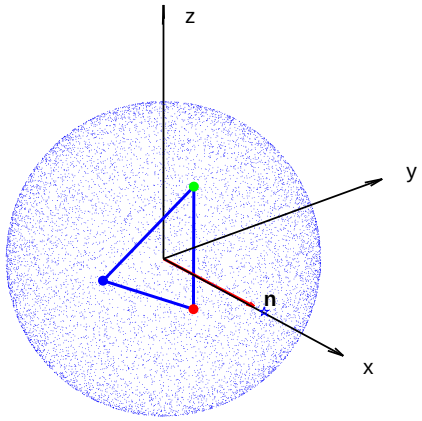

Figure 14: Best initial configuration

which is nearly equal to the ideal condition of unchanged shape and size of the formation.

As explained in the previous paragraphs, performance is evaluated only at the end of the period, without considering the evolution of the formation along the reference orbit. At this point it is interesting to look at the behavior of the formation while it orbits near the reference path.

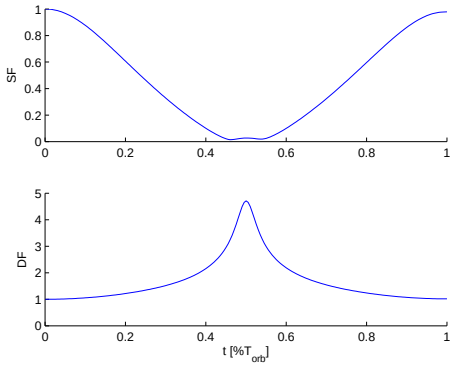

Figure 15: SF (top) and DF (bottom) behavior in time during one orbit - best initial configuration case

Figure 15 shows the time behavior of the two performance factors during a complete orbital period. Note that the two functions oscillates with the

same period of the orbit, reaching the lowest performance nearly at half orbit. At that point, the triangle collapses nearly onto a line (Figure 16), but finally it got back to almost its initial configuration (Figure 17).

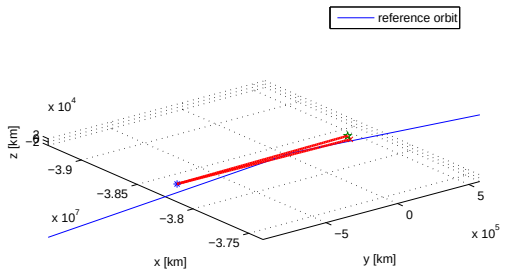

Figure 16: Triangular formation after half period

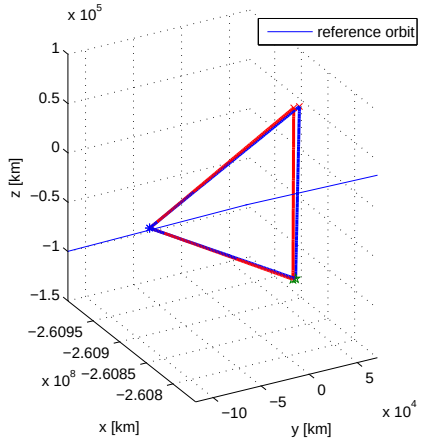

Figure 17: Comparison between initial (red) and final (blue) formation, after one period

It is important to remark that only free dynamics is considered here, meaning that the formation after one orbit comes back to its initial configuration without any control action, but only through a convenient exploitation of the dynamics of the elliptic three-body system.

5. Conclusion

The paper studies the free dynamics of an equilateral triangular formation of spacecraft under the Circular and Elliptic Restricted Three-Body Problem formulation. Its dynamics have been investigated by considering several initial configurations sets, in terms of orientation, size and location of the formation with respect to the three-body synodic frame. To quantify and compare formation keeping performance, two performance factors have been built: the shape and size changes of the triangular formation have been monitored and suitable initial configurations of the formation, leading to convenient solutions, in terms of formation keeping performance, have been identified. Two levels of study have been performed to understand the general dependency and influence of design variables on formation keeping performance in CR3BP and ER3BP.

The results of the study highlight that within the domain of study, performance is not dependent on the size of the triangle, while it strongly depends on the initial orientation and on the reference orbit the formation is orbiting about. For these reasons, when designing such kind of missions, to lower formation keeping needs to be provided to the three spacecraft, the initial orientation and reference orbit of the formation must be chosen carefully. As far as the present study is concerned, the best results have been achieved for formations orbiting about L3, and in particular when the triangle lies initially on the y, z plane of the synodic reference frame, with one spacecraft initially on the x, y plane.

References

[1] B. T. Barden, H. K. C, Formation flying in the vicinity of libration point orbits, AAS 98-169.

[2] G. Gómez, M. Marcote, J. J. Masdemont, J. M. Mondelo, Natural configurations and controlled motions suitable for formation flying, AAS 05-347.

[3] A. Héritier, K. C. Howell, Regions near the libration points suitable to maintain multiple spacecraft.

[4] F. Ferrari, M. Lavagna, Formation flying and relative dynamics under the circular restricted three-body problem formulation, in: Spaceflight

Mechanics 2014, Roby S. Wilson et al. (Eds.), Santa Fe, NM, USA, 2014, pp. 185–204.

[5] M. Bando, A. Ichikawa, Periodic orbits and formation flying near the libration points.

[6] J. J. C. M. Bik, P. N. A. M. Visser, O. Jenrich, Stabilization of the triangular lisa satellite formation.

[7] J. J. Guzmán, A. Edery, Mission design for the mms tetrahedron formation, IEEEAC.

[8] J. Dow, S. Matussi, R. Mugellesi Dow, M. Schmidt, M. Warhaut, The implementation of the cluster ii constellation, Acta Astronautica 54 (2004) 657–669.

[9] V. Szebehely, G. E. O. Giacaglia, On the elliptic restricted problem of three bodies, The Astronomical Journal 69 (3).

[10] P. Gurfil, D. Meltzer, Stationkeeping on unstable orbits: Generalization to the elliptic restricted three-body problem, The Journal of the Astronautical Sciences 54 (1).

[11] R. Broucke, Stability of periodic orbits in the elliptic, restricted three-body problem, AIAA Journal 7 (6) (1969) 1003–1009.

[12] S. Campagnola, M. Lo, P. Newton, Subregions of motion and elliptic halo orbits in the elliptic restricted three-body problem, in: Proceedings of 18th AAS/AIAA Space Flight Mechanics Meeting, Galveston, TX, USA, 2008.